Journal of Colloid and Interface Science **243,** 143–155 (2001)
doi:10.1006/jcis.2001.7885, available online at http://www.idealibrary.com on IDEAL®

Changes in the Morphology of Self-Assembled Polystyrene Microsphere Monolayers Produced by Annealing

Christian Gigault,[1] Kari Dalnoki-Veress,[2] and John R. Dutcher[3]

Department of Physics and Guelph-Waterloo Physics Institute, University of Guelph, Guelph, Ontario, Canada N1G 2W1

Received January 22, 2001; accepted July 26, 2001; published online September 20, 2001

Ordered monolayers of polystyrene (PS) microspheres were prepared on both hydrophilic and hydrophobic substrates by convective self-assembly. Changes in the degree of ordering in the microsphere monolayers during annealing at temperatures below and above the glass transition temperature T_g of PS was quantitatively assessed using a customized image analysis method. This method overcomes the shortcomings of traditional Fourier transform methods for the analysis of images containing a small number of objects. In general, large ordered domains in the monolayers break up into smaller regions separated by cracks, due to thermal expansion of the polymer and the attractive dispersion force between microspheres. The substrate influences this phenomenon: the evolution was much slower for instance for monolayers on glass than for monolayers on PMMA substrates. In annealing experiments above T_g of PS, measurements of the widths of cracks in the monolayers showed differences between substrates: At later stages the width of the cracks in monolayers on PS substrates were observed to decrease more quickly than for monolayers on PMMA substrates. After very long times at relatively high temperatures, the monolayers on both substrates became essentially smooth films.

Key Words: **microsphere monolayers; self-assembly; morphology; annealing; image analysis.**

1. INTRODUCTION

Recently, there has been considerable interest in the self-assembly of ordered crystals of polymer microspheres (1–4). If a drop of a suspension of polymer microspheres is allowed to dry on a substrate, the flow that is driven by evaporation of the suspending liquid will result in the accumulation of microspheres near the periphery of the drying drop (1), self-assembling into a mixture of ordered and disordered regions. Several methods have been developed to produce dry ordered microsphere mono- and multilayers. These methods include field-induced layering (2), in which microspheres in a water suspension are deposited onto a substrate by applying an electric field perpendicular to the plane of the substrate, so-called micromolding in capillaries (3), in which the microspheres flow through channels in a prefabricated micromold; and the method of convective self-assembly, in which the flow of water caused by evaporation causes the microspheres to self-assemble onto a substrate in an ordered way. Using convective self-assembly, it is possible to generate large (areas of several square millimeters), highly ordered monolayers on hydrophilic substrates (4). The main criterion for generating highly ordered monolayers is for the top surface of the suspension to form a concave meniscus which assures that the suspension dries from the central region outward, leaving microspheres adsorbed to the central region of the substrate. Under the proper conditions, large, highly ordered microsphere monolayers are obtained.

In the present study, we have used convective self-assembly to prepare polystyrene (PS) monolayers on hydrophilic substrates, such as glass and mica, and we have used a modified convective self-assembly technique to prepare PS monolayers on hydrophobic substrates, namely PS and poly (methyl methacrylate) (PMMA) films on silicon wafers. Using reflected-light microscopy, we have characterized the changes in the morphology of the monolayers produced by annealing. In general, one might expect to observe changes in the ordering when the monolayers are heated to temperatures greater than the glass transition temperature T_g of the PS microspheres. Surprisingly, we observed large changes in the monolayer morphology by annealing to temperatures *below* the T_g of PS. Cracks were observed to form between small, highly ordered monolayer regions, which can be explained qualitatively in terms of the attractive dispersion force between adjacent microspheres. We have also tracked the changes in morphology produced by annealing to temperatures above the T_g of PS, and we find qualitatively different behavior in the annealed PS microsphere monolayers for different substrates.

2. SAMPLE PREPARATION

Polystyrene (PS) microsphere monolayers were prepared using an aqueous suspension of (1.02 ± 0.02) μm charge-stabilized microspheres (5), diluted from the original stock suspension with deionized water to a mass fraction of 0.005.

[1] Present address: JDS Uniphase Corporation, 570 West Hunt Club Road, Nepean, Ontario, Canada K2G 5W8.

[2] Present address: Department of Physics and Astronomy, McMaster University, Hamilton, Ontario, Canada L8S 4L8.

[3] To whom correspondence should be addressed. E-mail: dutcher@physics.uoguelph.ca.

0021-9797/01 $35.00

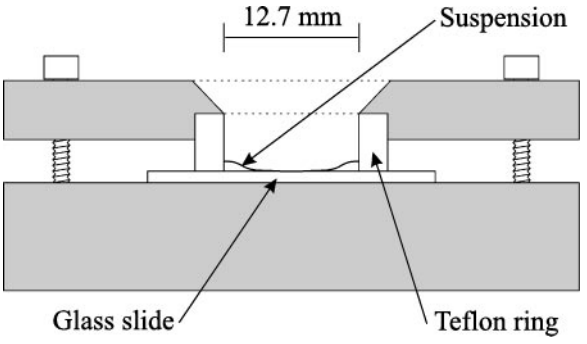

FIG. 1. Convective self-assembly evaporation cell. The diameter of the cylindrical opening in the PTFE piece is 12.7 mm and the height is 4 mm. A 50-μl volume of an aqueous suspension of polystyrene microspheres (mass fraction 0.005) has been deposited in the cell and the figure shows the approximate shape of the liquid surface.

Large domains (with areas of a few mm^2) of monodisperse microspheres were prepared on hydrophilic substrates (premium quality glass slides (6)) using the method of convective self-assembly, which has been described in detail previously (4, 7). Immediately before use, the slides were rinsed with xylene and acetone, and subsequently immersed in a 15% hydrofluoric acid solution for 10 s. The last step ensures that the slides, after being rinsed abundantly with deionized water, are hydrophilic. Typically 50 μl of suspension was deposited in a cell consisting of a cylindrical poly (tetrafluoroethylene) (PTFE) enclosure pressed against the glass substrate (see Fig. 1). PTFE was chosen because its wetting properties are such that a concave meniscus formed at the center of the cell.

We inferred from observation of the self-assembly process using a microscope that the microspheres are driven by the convective flow of water with forces that are much larger than the electrostatic repulsion of the charge-stabilized microspheres, and the morphology of the ordered array is largely determined by the convective flow. After the water has evaporated, the microspheres are electrically neutral and are no longer repelled by each other.

The method of convective self-assembly, as described in Refs. (4, 7), only works well on hydrophilic substrates. The contact angle for drops of the microsphere suspension in water deposited on PS films on Si (PS substrates) and on PMMA films on Si (PMMA substrates) was measured to be 83° and 69°, respectively. For these hydrophobic substrates, the liquid surface shape required for convective self-assembly to take place cannot be achieved, and samples prepared on such substrates using the method described in the previous section do not contain large ordered regions. Figure 2a is an image typical of the well-ordered regions of monolayers on hydrophilic glass substrates produced by convective self-assembly, and Fig. 2b is an image of the highest degree of order obtained in a sample prepared on a hydrophobic PMMA thin film on Si using the convective self-assembly process. The degree of ordering is obviously much less in the latter case.

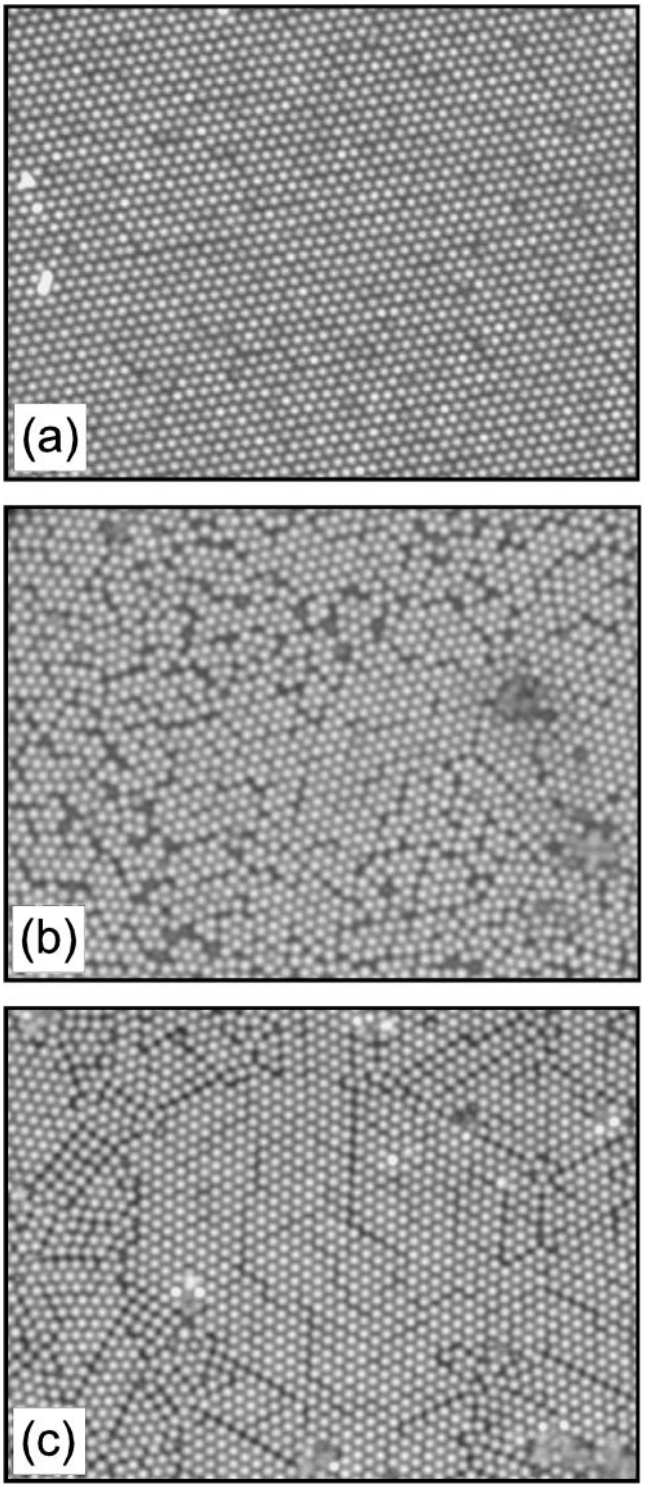

FIG. 2. Comparison between self-assembly on hydrophilic and hydrophobic substrates. (a) Image typical of the well-ordered areas of a monolayer of 1.02-μm microspheres self-assembled on a glass substrate. (b) Image of the best degree of ordering obtained for a monolayer self-assembled on a PMMA substrate using the same method as for hydrophilic substrates. (c) Image typical of well-ordered areas of monolayers on PMMA substrates, obtained using the modified self-assembly method. Images are approximately 51 μm $\times$ 38 μm in size.

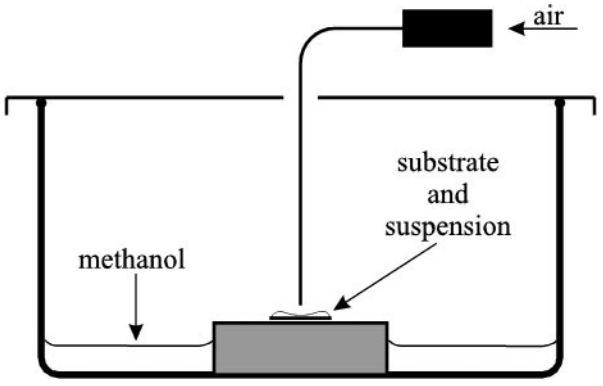

FIG. 3. Modified convective self-assembly cell used for hydrophobic substrates.

We have modified the convective self-assembly method to allow the fabrication of well-ordered monolayers on the hydrophobic PS and PMMA substrates using the following procedure. Some of the aqueous suspension of PS microspheres was thoroughly dried, and the microspheres were then resuspended in methanol to make 0.002 mass fraction suspensions. Methanol was chosen for two reasons: it wets polymers like PMMA considerably better than does water, with contact angles $<5^\circ$; and it does not dissolve the PS microspheres. Since the evaporation rate of methanol is much larger than water, the sample preparation was performed in an atmosphere saturated with methanol, to slow down the evaporation rate such that good-quality monolayer areas could self-assemble. The substrate was placed onto a piece of aluminum sitting in methanol at the bottom of a glass vessel fitted with a lid through which passed a 0.7-mm hollow steel tube. The tube was connected to a compressed air supply, allowing a very small flow of air to be directed onto the sample center (see Fig. 3). A cylindrical enclosure, such as the PTFE enclosure used to achieve the necessary concave meniscus shape in the conventional convective self-assembly procedure, could not be used with the polymer film substrates. Such an enclosure could not be placed in contact with the PS and PMMA substrates because this would damage the polymer films, allowing the methanol to penetrate between the polymer film and the underlying Si substrate. The microsphere suspension ($20\,\mu$l) in methanol was deposited on the substrate through the small hole in the lid, and the steel tube was immediately placed through the hole. Air flow was adjusted to obtain a slightly concave surface in the center of the suspension, allowing the self-assembly to begin there. Figure 2c is an image typical of the well-ordered areas obtained using the modified self-assembly method. The quality of the order is much better in Fig. 2c than in Fig. 2b.

Microsphere monolayers were fabricated using the modified self-assembly method on thick films ($\sim$150 nm) of PS ($M_w = 727 \times 10^3$, $M_w/M_n = 1.1$ (8)) and PMMA ($M_w = 1.2 \times 10^6$, $M_w/M_n = 1.39$ (8)) spin coated onto 9 mm $\times$ 9 mm, 0.5-mm-thick Si squares cut from a 76.2-mm (3″) Si(001) wafer (9). The thickness of the PS and PMMA films, which was chosen to be large enough to suppress the van der Waals interaction between the PS microspheres and the Si substrate (10), was measured using ellipsometry.

3. MICROSCOPE SYSTEM AND IMAGE ANALYSIS

The video microscopy system was based on an Olympus BX60 microscope equipped with a long-working-distance 50$\times$ objective. A Sony DXC-950 3-CCD color camera was attached to the microscope via a 2.5$\times$ camera adapter. True-color (640 $\times$ 480 pixel, 24-bit) bitmap images were acquired using an Integral Technologies Flashpoint 128 frame grabber and subsequently processed and analyzed using the software package Image–Pro Plus (11) and various C++ programs that were written to perform specific steps in the analysis.

The spatial calibration of the images was performed by imaging a precision diffraction grating with (600 $\pm$ 1) grooves/mm, and was therefore accurate to within approximately $\pm$0.2%. With the 50$\times$ objective and 2.5$\times$ camera adapter, the calibration was found to be (12.66 $\pm$ 0.02) pixels/μm in both the horizontal and vertical directions.

For the annealing experiments, a home-built hot stage was attached to the microscope sample stage. Samples were observed in reflected light through a window (0.17-mm glass cover slip) on the hot stage. The objective of the microscope was not corrected for the thickness of such a window; however, only a slight reduction in contrast was observed in images collected with the window compared with those collected without the window.

The temperature, measured with a type T thermocouple in contact with the sample, was controlled using a Eurotherm 808 temperature controller, and was accurate to within $\pm 0.5^\circ$C. The mechanical stability of this setup was such that for constant-temperature annealing experiments, the correct focus could be maintained without adjustment for periods of time up to a few hours. However, the focus had to be continuously adjusted during annealing experiments in which the temperature was ramped, because of thermal expansion within the hot stage.

The spatial coordinates derived from the verniers on the X–Y translation stage of the microscope were accurate enough, even at high magnification, to allow the return to a particular area of the sample that had been imaged previously. This allowed the tracking of multiple regions of the microsphere monolayers, which was essential to the morphology studies described below.

A typical microsphere monolayer image consisted of a two-dimensional array of bright circular regions corresponding to the individual microspheres. Typically, the monolayers contain small, densely packed regions surrounded by gaps, or “cracks” (see Fig. 2c). To extract quantitative information about the two-dimensional ordering and the distribution of nearest-neighbor distances, Fourier transform methods are traditionally used. In principle all the information about an image is contained in its Fourier transform but in practice it is not easy to extract from Fourier transforms of images like that shown in Fig. 2c

information about the ordering inside small, densely packed regions, or information about cracks.

An image analysis procedure was developed which overcomes the shortcomings of Fourier transform methods for the analysis of images containing a small number of objects like the images shown in this article (and images such as those shown in Refs. (12, 13)). The procedure extracts the coordinates of all microspheres present in the image, identifies all nearest-neighbor pairs, and is well suited for automation in a computer program. Tabulation of statistics like average nearest-neighbor distances is then possible. For images of monolayers fabricated with microspheres of diameters of the order of 1 μm, on opaque or transparent substrates, it was found that very good contrast was obtained by using only the green channel of the RGB images. This results in grayscale images having in their raw form an 8-bit pixel depth.

The method used to obtain the (x, y) coordinates of the microspheres present in an image is based on that used in Ref. (14). The authors analyzed images containing microspheres that were separated by distances larger than their diameter. For these images, in which the background between microspheres could be subtracted, a simple centroid method was used to refine the initial coordinate estimates: the fractional corrections δ_x and δ_y to be applied to an initial estimate (x, y) were computed by calculating the "center of mass" of the brightness in a region with a radius comparable to the microsphere size centered around (x, y) in the filtered image (14). However, in the case of a closed packed array, simply weighting the pixels by their intensity value is not sufficient because there is a nonzero, slowly varying background in the image that cannot be subtracted, and the results of the centroid method would be heavily biased toward the center of the region considered. Since the center of the region is the initial estimate itself, values of δ_x and δ_y that are essentially zero would be returned. Instead, we used a modified centroid method where pixels are weighted according to some power m of the brightness value:

$$\delta_x = \frac{1}{M} \sum_{i^2+j^2 \le w^2} i \times (I'_{x+i,y+j})^m, \qquad [1]$$

$$\delta_y = \frac{1}{M} \sum_{i^2+j^2 \le w^2} j \times (I'_{x+i,y+j})^m, \qquad [2]$$

where I' is the filtered image and the normalization constant M is given by

$$M = \sum_{i^2+j^2 \le w^2} (I'_{x+i,y+j})^m. \qquad [3]$$

Good results were obtained using $m = 4$ and $w = 4$.

Following the calculation of a list of the coordinates of each microsphere, quantities such as the average and standard deviation of the microsphere-to-microsphere distance, and the sixfold bond orientation order parameter ψ_{6j} (15), were computed. In order to automate the process, the systematic selection of nearest-neighbor pairs was performed using the Delaunay triangulation procedure, which is the dual of the Voronoi polygon tessellation (16).

4. EXPERIMENTS BELOW T_g OF PS

Although it is expected and observed (see below) that changes to the microsphere monolayers will occur at temperatures above the glass transition temperature T_g of the PS microspheres and the PS and PMMA substrates (97°C and 100°C, respectively (17)), we also observed that the morphology of microsphere monolayers could change noticeably as the temperature was ramped from room temperature up to a temperature well below the glass transition temperature T_g of PS and PMMA. For samples in which the initial degree of close-packed ordering was poor, no change in the monolayer morphology was observed upon annealing. However, when samples with higher initial degrees of close-packed ordering were annealed, microspheres would move and a large, apparently well-ordered domain would break up into a collection of smaller domains separated by cracks, similar to the appearance of a dried mud puddle. Figure 4 illustrates this behavior for a self-assembled microsphere monolayer on a PMMA substrate.

The rearrangement of the microspheres within the monolayers can be understood in terms of the initial degree of disorder within the monolayer. The process of self-assembly of the microsphere monolayers does not generate perfect two-dimensional crystals. Rather, some amount of disorder is "frozen in," and inside a fairly well-ordered domain, the average microsphere-to-microsphere distance is slightly larger than the microsphere diameter. As the temperature increases, the microspheres expand and the distance between the surfaces of adjacent microspheres decreases. This occurs because the thermal expansion coefficient of PS ($\sim 7 \times 10^{-5}$ K^{-1} below T_g (17)) is approximately 30 times larger than it is for Si (2.33×10^{-6} K^{-1} (18)) and therefore, to a very good approximation, the substrate area occupied by the monolayer essentially does not change as the temperature is increased (polymer films on Si substrates are also similarly constrained, and thermal expansion occurs for these films only in a direction normal to the surface of the substrate). Microspheres in air do not experience the electrostatic repulsion present when the microspheres are suspended in water, and as the surfaces of adjacent microspheres approach each other, the short-range attractive dispersion force between the microspheres becomes larger and the microspheres can "stick" to each other. Regions that initially are more densely packed will become even denser, and they will be separated from other such regions by gaps, which correspond to the dark cracks visible on Fig. 4b. When the temperature is decreased to room temperature, microspheres become smaller, but if the surfaces of neighboring microspheres stick together during the heating cycle, this will be maintained as the temperature is decreased, forming small, densely packed regions within the monolayer. Correspondingly, the cracks become wider as the temperature is decreased.

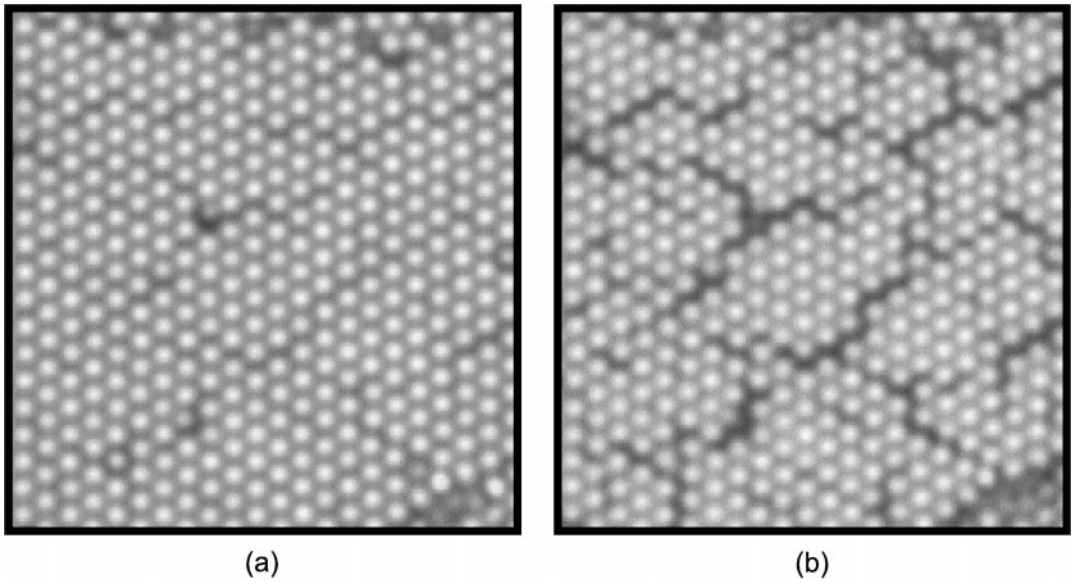

FIG. 4. Image of a small area of a monolayer of 1.02-μm PS microspheres on a 145-nm PMMA film on Si. (a) Initial state at 20°C, and (b) at 90°C after ramping at a rate of 1°C/min.

To test the hypothesis that after a long annealing time below T_g the most densely packed regions will reach a maximum packing density corresponding to the closely spaced microspheres sticking to their neighbors, several small regions of a monolayer self-assembled on a 150-nm PMMA film on Si which had been held at 90°C for 12 h were imaged at high magnification with the temperature fixed at 90°C, and then reimaged after the monolayer was cooled to room temperature (20°C). For a number of small, densely packed regions, the average microsphere-to-microsphere distance $\bar{a}$ was computed in the manner described in Section 3. Figure 5 shows one of many 640×480 pixels images obtained, and one of the small, densely packed regions chosen within the larger image. Microspheres that were not to be included in the densely packed region had to be masked out to prevent their identification by the detection algorithm.

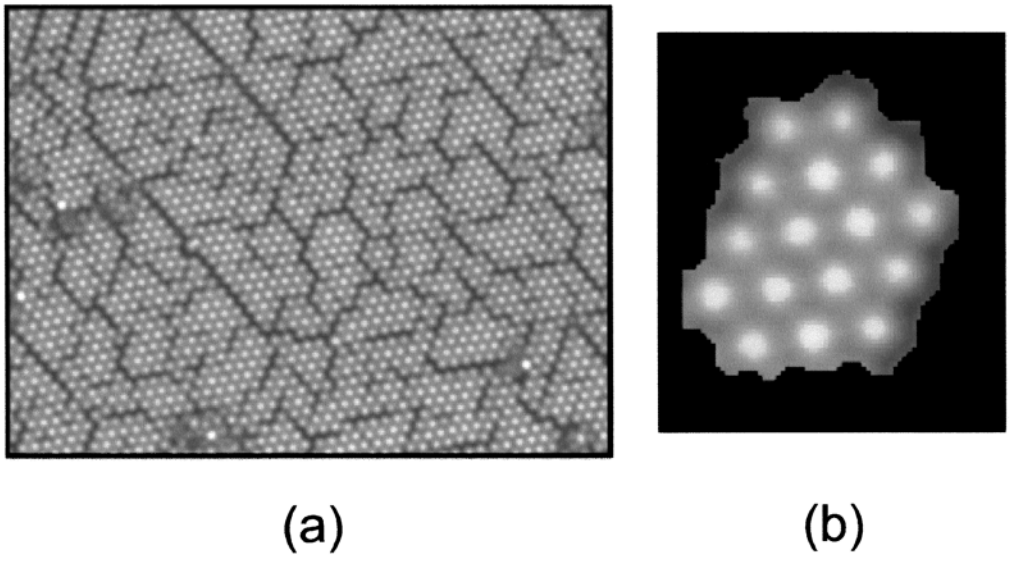

FIG. 5. (a) Image of a 1.02-μm microsphere monolayer on PMMA, at 90°C. Grayscale image obtained from the green RGB channel of original image. (b) Detail of image in (a), in which microspheres that are not to be included in the densely packed region have been masked out. Calibration of images: 12.66 pixels per μm.

TABLE 1

Summary of Average Microsphere-to-Microsphere Distance Measurements at 90° and at 20°C Computed from a Total of 553 Microsphere-to-Microsphere Distance Measurements

	$\bar{a}$ (μm)	σ_a (μm)
90°C	1.0148	0.0014
20°C	1.0108	0.0013
Difference	0.004	0.0019
Thermal expansion	0.0049	—

Table 1 summarizes the comparison between the microsphere monolayer morphology obtained after annealing at 90°C for 12 h and that obtained after cooling to room temperature. The difference between the average microsphere-to-microsphere distance at the two temperatures is significant, and is equal within experimental uncertainty to the result expected on the basis of thermal expansion: If one uses the published value for the coefficient of thermal expansion for glassy PS, 7×10^{-5} K^{-1} (17), and a temperature difference of 70°C, one obtains a decrease in size of approximately 0.0049 μm. Note that with the image calibration of 12.66 pixels/μm, this statistically significant measured difference amounts to approximately 1/20th of a pixel.

In addition, the average microsphere-to-microsphere distance corresponds to the microsphere diameter. Considering the uncertainty on the calibration of images obtained with the microscope (approximately ±0.2%, or ±0.002 μm for a measurement of 1 μm, see Section 3), the value of 1.0108 μm at 20°C is equal within experimental uncertainty to the value quoted by the manufacturer, 1.02 μm with a standard deviation of 0.02 μm.

We have also compared the average microsphere-to-microsphere distance for densely packed regions, measured at room temperature before annealing, to the average microsphere-to-microsphere distance for the same densely packed regions, measured at room temperature after annealing the sample. The annealing history of the samples consisted of ramping the temperature from 20° to 90°C at 1°C per min, holding the samples at the elevated temperature for a certain amount of time, then ramping the temperature back down to 20°C at the same rate. In Fig. 6, we plot the average microsphere-to-microsphere distance after annealing versus the average microsphere-to-microsphere distance before annealing obtained for a large number of densely packed regions in a PS microsphere monolayer on a glass substrate. The sample was heated at 1°C per min from 20° to 90°C, and then immediately cooled at 1°C per min to 20°C . Each data point in Fig. 6 corresponds to a different, small, well-ordered region of the monolayer, and the solid line corresponds to unity slope. The data points essentially coincide with the solid line, indicating no change for this annealing cycle in the average microsphere-to-microsphere distance for the sample.

Figure 7 shows the same type of plot as in Fig. 6, obtained for the same areas of the same sample as in Fig. 6 after heating

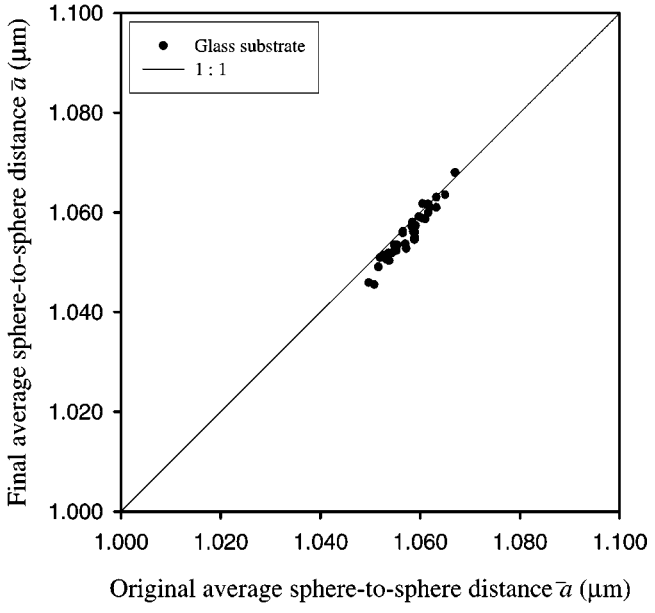

FIG. 6. Average microsphere-to-microsphere distance after annealing versus initial average microsphere-to-microsphere distance, for a 1.02-μm microsphere monolayer sample on a glass substrate. Annealing was done by ramping temperature from 20° to 90°C, then immediately back to 20°C, at 1°C per min.

the sample from 20° to 90°C at 1°C per min, holding the sample at 90°C for 12 h, and then cooling the sample at 1°C per min to 20°C. The data points clearly lie below the solid line, indicating a decrease in the average microsphere-to-microsphere

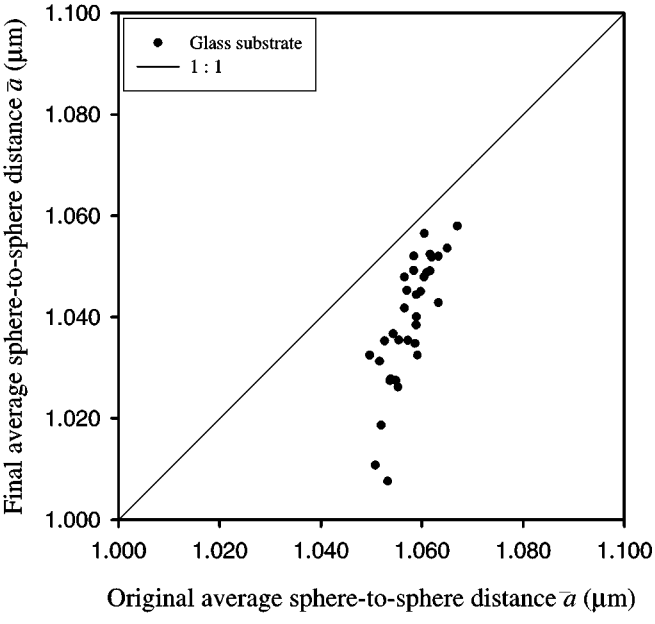

FIG. 7. Average microsphere-to-microsphere distance after annealing versus initial average microsphere-to-microsphere distance (before all annealing cycles), for the same areas as in Fig. 6, after a subsequent annealing cycle which included a 12-h plateau at 90°C.

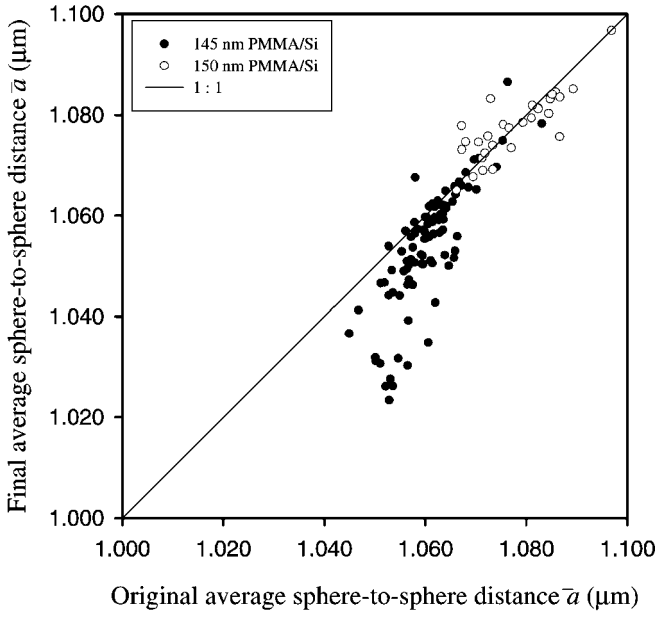

FIG. 8. Average microsphere-to-microsphere distance after annealing versus initial average microsphere-to-microsphere distance, for two 2.02-μm microsphere monolayer samples on PMMA substrates. The annealing cycle consisted of ramping temperature from 20° to 90°C, then immediately back to 20°C, at 1°C per min.

distance after an extended annealing time at 90°C. In addition, the smaller the value of the original average microsphere-to-microsphere distance, the larger the decrease in its value after annealing. This is consistent with the interpretation in

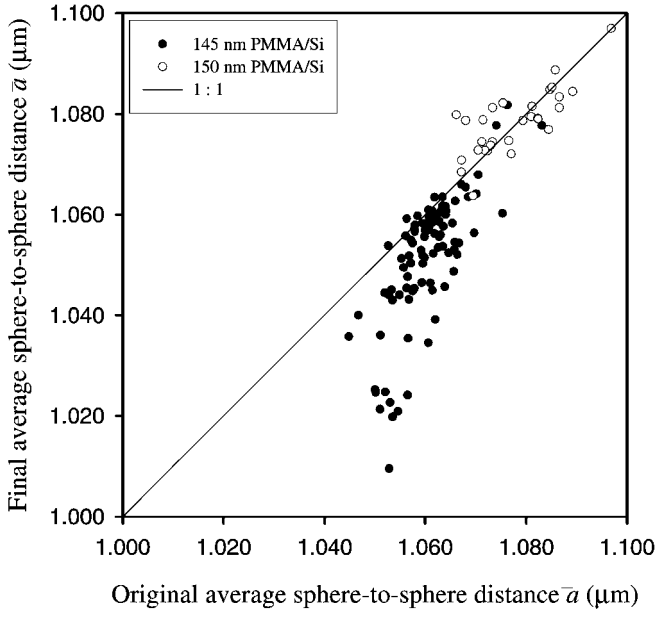

FIG. 9. Average microsphere-to-microsphere distance after annealing versus initial average microsphere-to-microsphere distance (before all annealing cycles), for the same areas as in Fig. 8, after a subsequent annealing cycle which included a 30-min plateau at 90°C.

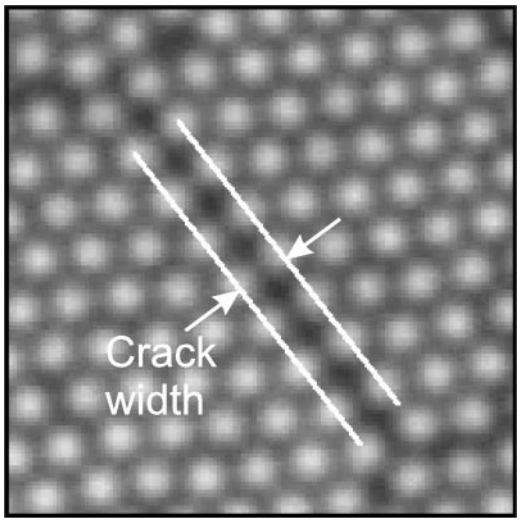

FIG. 10. "Crack" separating densely packed regions, in a monolayer on a 145-nm-thick PMMA film on a Si substrate. The width of the crack is defined as the perpendicular distance between lines joining the centers of microspheres on each side of the crack (white lines on the figure).

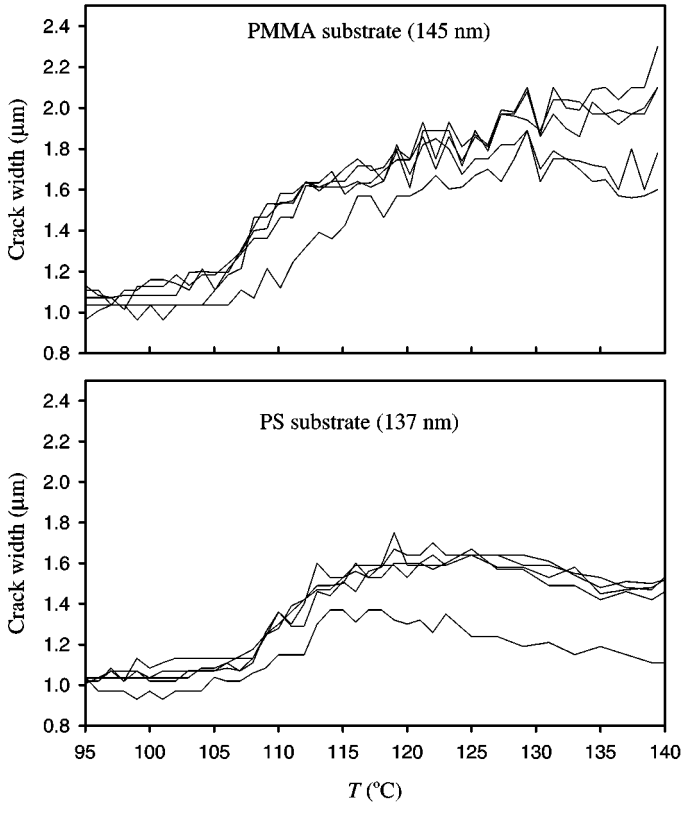

FIG. 11. Widths of several cracks separating densely packed regions, in a monolayer of 1.02-μm microspheres on a 145-nm-thick PMMA film on Si substrate and in a monolayer on a 137-nm-thick PS film on Si, as a function of temperature. The temperature was ramped from 95° to 140°C at a rate of 1°C per min.

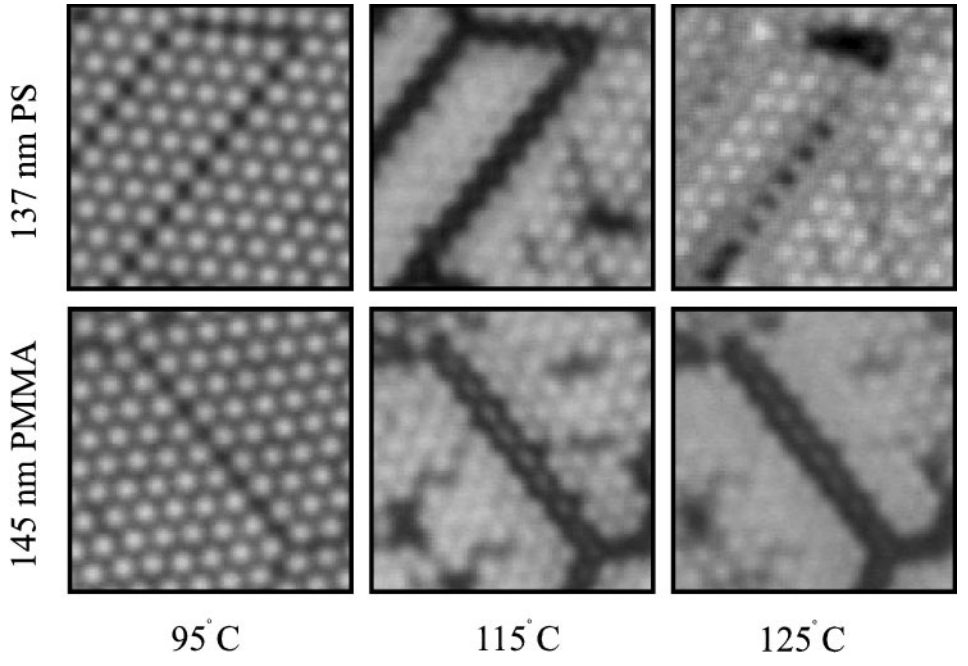

FIG. 12. Images of a monolayer of 1.02-μm PS microspheres on a 137-nm PS/Si substrate and on a 145-nm PMMA/Si substrate during annealing above T_g.

terms of short-range attractive forces between the microspheres which cause decreases in the microsphere separation only for regions in which microspheres were initially very close together.

The nature of the substrate affected the rate at which changes in the microsphere monolayer morphology occurred at elevated temperatures. In experiments performed with microsphere monolayers on PMMA substrates, the decrease in

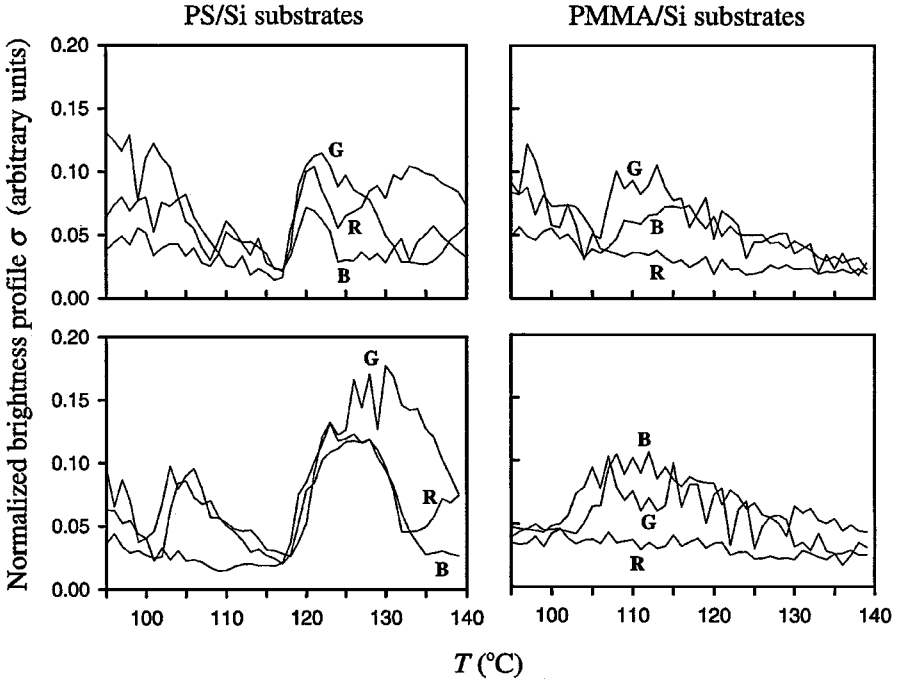

FIG. 13. Standard deviation of the pixel brightness profile along a line coinciding with the center of a crack, for four different samples: two monolayers on PS/Si substrates, and two monolayers on PMMA/Si substrates. The temperature was ramped from 95° to 140°C at a rate of 1°C per min. The standard deviation has been normalized to the whole image average grayscale brightness. R, G, and B stand for the red, green, and blue channels, respectively.

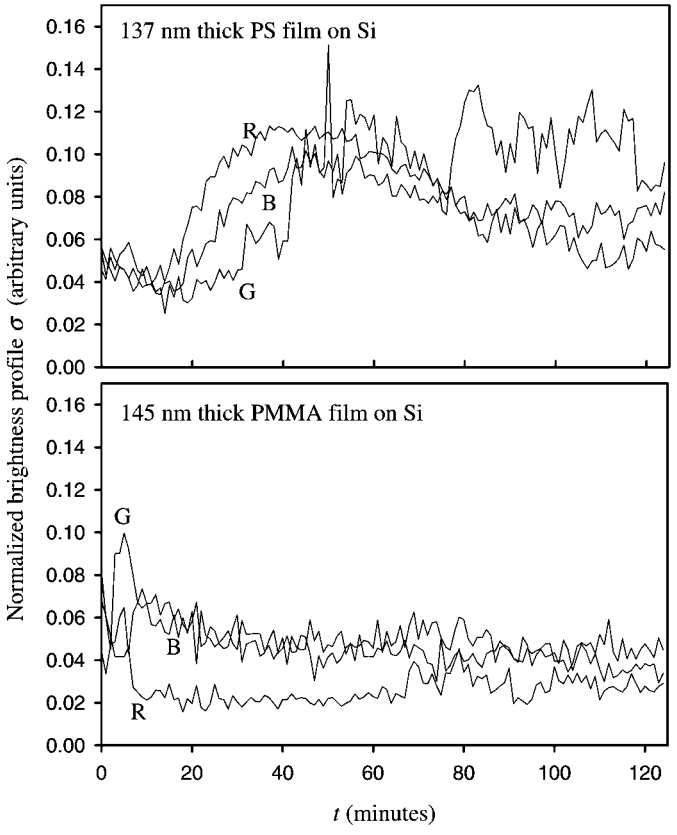

FIG. 14. Standard deviation of the pixel brightness profile along a line coinciding with the center of a crack, for a monolayer on a PS/Si substrate and a monolayer on a PMMA/Si substrate, at a temperature of 110°C. The standard deviation has been normalized to the whole image average grayscale brightness. R, G, and B stand for the red, green, and blue channels, respectively.

microsphere-to-microsphere distance occurred much faster than on glass substrates. In Fig. 8 is shown the data obtained for two microsphere monolayers on PMMA substrates after annealing cycles that were identical to that used to obtain the data for the microsphere monolayer on the glass substrate shown in Fig. 6: The temperature was ramped up to 90°C, then immediately back down to room temperature. In contrast to the absence of change in the microsphere monolayer morphology observed for the glass substrate for this brief annealing cycle, for the PMMA substrate there are substantial decreases in the final average microsphere-to-microsphere distances compared with the original values for areas of the monolayers with an average microsphere-to-microsphere distance smaller than a certain critical value ($\sim$1.07 μm). For areas of the monolayers on the PMMA substrates with an average microsphere-to-microsphere distance greater than the critical value, the final average microsphere-to-microsphere distance was essentially the same as the original one, which is consistent with the interpretation in terms of short-range attractive forces between the microspheres. Figure 9 shows the data obtained for the same areas of the same two microsphere monolayers on PMMA substrates as for Fig. 8, after heating the samples from 20° to 90°C at 1°C per min, holding the samples at 90°C for 30 min, and then cooling the samples at 1°C per min to 20°C. There are further small decreases in the average microsphere separation following the second annealing cycle, such that the changes in the microsphere monolayer morphology on the PMMA substrates shown in Fig. 9, obtained after annealing at 90°C for 30 min, are comparable to the changes in the microsphere monolayer morphology on the glass substrate only after annealing at 90°C for much longer times (see Fig. 7). However, most of the changes in the microsphere monolayer morphology on the PMMA substrates have occurred during the first brief annealing cycle, and the effect is much larger than that observed for the glass substrates.

The set of original average microsphere-to-microsphere distances for the monolayers on the glass substrate contained microsphere separations as small as those observed for the monolayers on PMMA substrates (for instance, the black circles on

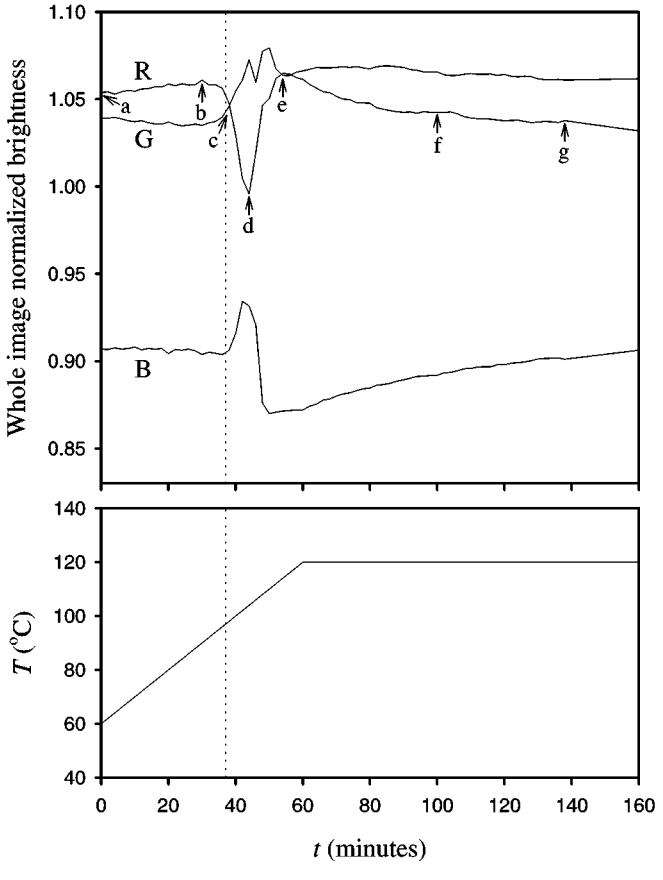

FIG. 15. Color contents of images acquired during the annealing of a 1.02-μm microsphere monolayer on a glass slide. The color brightness values were normalized to the whole-image average grayscale intensity. The letters R, G, and B refer to the red, green, and blue contents of the image, and the lowercase letters indicate the times at which the images shown in the various panels of Fig. 16 were acquired. The dotted line indicates the time at which the temperature is equal to 97°C, the glass transition temperature for PS.

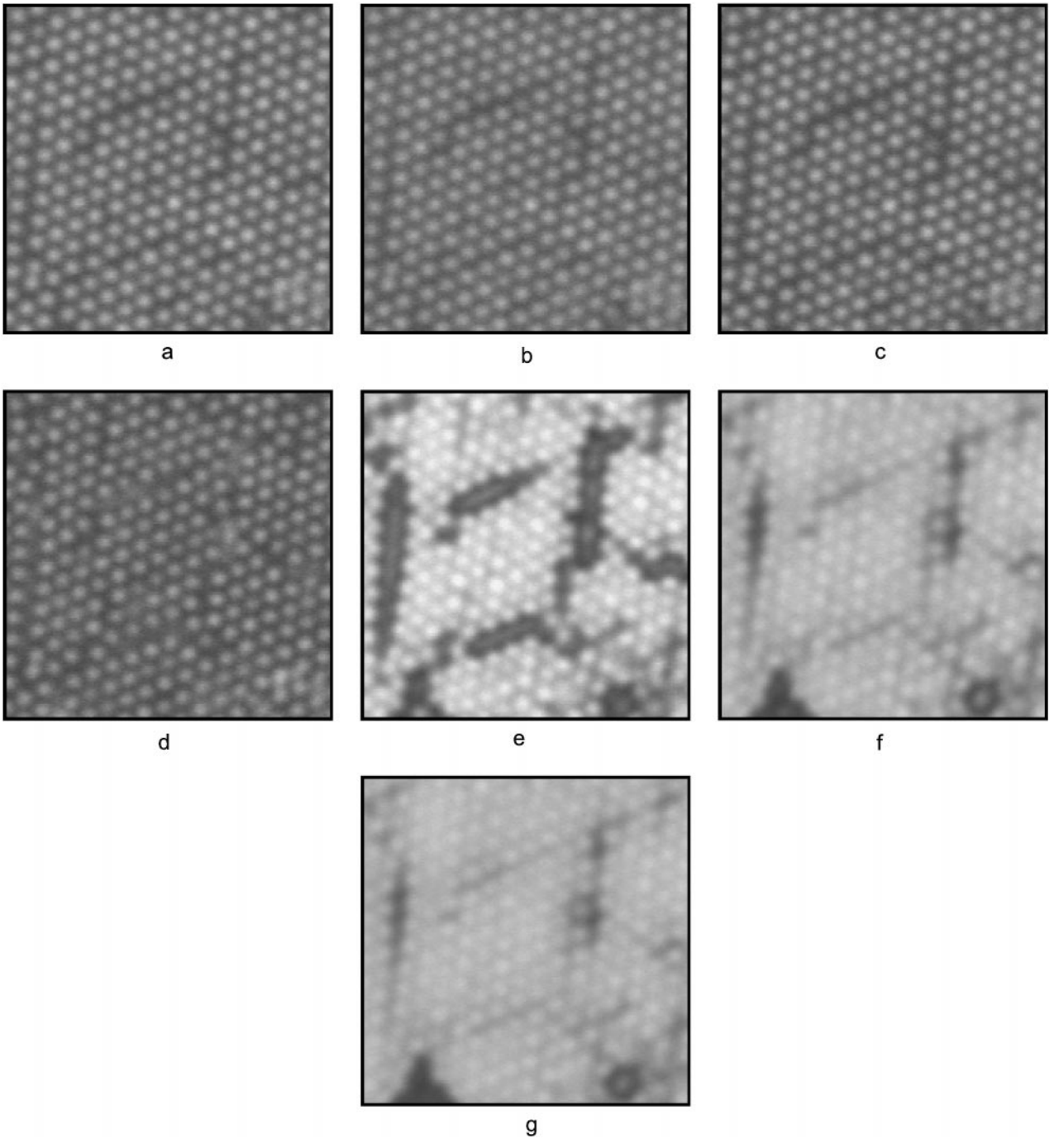

FIG. 16. Images acquired during the annealing of the 1.02-μm microsphere monolayer on a glass slide. The color images were converted to grayscale. The letters correspond to those in Fig. 15.

Fig. 8), and yet the evolution of the microsphere-to-microsphere distance was much slower for the glass substrate than it was for the PMMA substrate.

The force responsible for pulling the electrically neutral microspheres toward each other must be effective only over distances of the order of 40 nm, which is the largest difference in the separation of the microsphere surfaces for which morphology changes are observed (cf. Figs. 7 and 9). This distance is an order of magnitude larger than the increase in the size of the microspheres of approximately 4 nm which occurs in the present experiments due to thermal expansion. The interaction energy U between two microspheres due to the (nonretarded) dispersion

force (19) is given by

$$U(D) = -\frac{A}{6D}\frac{r_1 r_2}{r_1 + r_2}, \quad [4]$$

where A is the Hamaker constant, D is the separation between microsphere surfaces, and r_1 and r_2 are the radii of the microspheres. The corresponding attractive force F for two identical microspheres of radius $r = d/2$ is given by

$$F = -\frac{dU}{dD} = \frac{Ad}{24D^2}. \quad [5]$$

For two polystyrene objects interacting through vacuum (or air), the Hamaker constant A is about 7×10^{-20} J (19), and two 1-μm microspheres separated by 40 nm are attracted by a force $F \sim 2 \times 10^{-12}$ N. For comparison, this is almost three orders of magnitude larger than the weight of such a microsphere (with density 1.05 g/cm^3), and we conclude that the decrease in microsphere-to-microsphere distance upon annealing is due to the attractive dispersion force. The situation is complicated by the presence of the underlying substrate. Because we observe a large difference in the dynamics of the morphology change for the glass and PMMA substrates, the influence of the substrate can be large. In addition, rolling or dragging of the microspheres can occur during the sticking of the microspheres at high temperature and during their subsequent cooling to room temperature, and this will be affected by the nature of the substrate. In principle, one should include retardation in the dispersion calculation because of the finite value of the speed of light, which has the effect of reducing the value of the Hamaker constant as D increases. However, for interactions across vacuum or air, retardation effects are not expected to be important for such small separations (19).

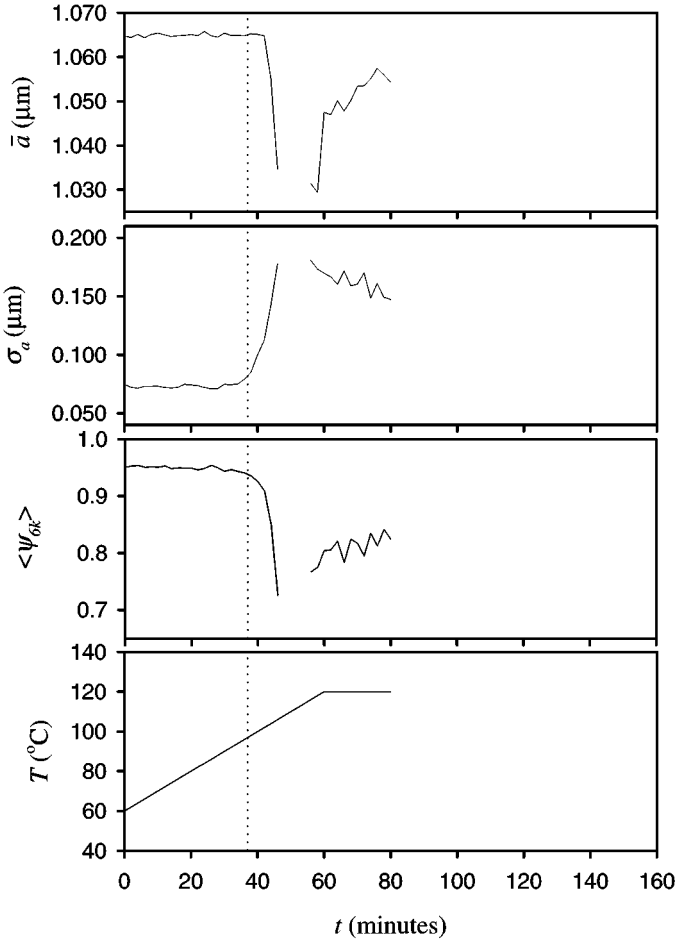

FIG. 17. Average microsphere-to-microsphere distance a, its standard deviation σ_a, and the average of the sixfold bond orientation order parameter, $\langle\psi_{6k}\rangle$, in images acquired during annealing of the 1.02-μm microsphere monolayer on a glass slide. The dotted line indicates the time when the temperature is equal to 97°C.

5. EXPERIMENTS ABOVE T_g OF PS

Annealing experiments were performed above the glass transition temperature T_g of polystyrene using the same experimental setup as in the previous section. The temperature was ramped at 1°C per min from 95° to 140°C, and images of the same area of the sample were acquired at 1-min intervals.

In the initial stages of the experiments, the changes in morphology for microsphere monolayers on PS, PMMA, and Si substrates did not differ significantly. Essentially there was no change at all until the temperature reached approximately 106°C, after which the cracks separating densely packed regions began to increase in width, as the microspheres in the densely packed regions started to deform and material began to flow.

The width of several such cracks was monitored as a function of time (and therefore temperature) by measuring the perpendicular distance between the two lines joining the centers of microspheres on each side of the crack (see Fig. 10). The results are shown in Fig. 11, for two different samples: a microsphere monolayer on a 145-nm-thick PMMA film on Si, and one on a 137-nm-thick PS film on Si. For each sample, the widths of five cracks were monitored.

It is only in the final stages of the annealing process that differences between the different substrates were apparent. Figure 12 shows images of a small area of a monolayer on a 137-nm-thick PS film on Si as well as images of a small area of a monolayer on a 145-nm-thick PMMA film on Si, at three temperatures during the annealing process. For both substrates, the cracks became wider as the temperature increased (images at 95° and 115°C). However, at a certain temperature for the monolayer on the PS substrates (at approximately 117°C when ramping at 1°C per min) the cracks started to fill in with material coming from what was left of the microspheres on each side of the crack, causing the sort of "ladder" morphology seen on the image taken at 125°C for the PS substrate. The spreading of the PS chains from the microspheres on the PS substrates is reasonable because of the compatibility of the polymer chains. The formation

of the ladder morphology did not occur for the PMMA/Si substrate which is reasonable because the PS and PMMA chains are immiscible.

To show graphically the difference between the two substrates, image pixel brightness profiles along a line coinciding with the center of a crack were obtained, for both monolayers on the PS and PMMA substrates, as shown in Fig. 13. If the brightness line profile has a periodic modulation, the standard deviation of the brightness will be proportional to the amplitude of the periodic modulation. In order to eliminate the effects of whole image brightness variations from image to image, the standard deviations of the line profiles were normalized to the whole-image average brightness. For the PS/Si substrates, there is a rapid increase in the standard deviation of the pixel brightness profile for all three color components at around 117°C, which corresponds to the onset of the filling of the cracks.

Alternatively, one can study the evolution of the crack morphology during annealing at a constant temperature above T_g. Annealing experiments were performed in which the temperature of a microsphere monolayer on a PS/Si substrate and a microsphere monolayer on a PMMA/Si substrate was ramped at 1°C per min from room temperature up to 110°C, and stabilized at that temperature. Figure 14 shows the standard deviation of the brightness along a line coinciding with the center of a crack, for both samples. The onset of the filling of the cracks occurred after approximately 15 min for the monolayer on the PS/Si substrate, and did not occur at all for the monolayer on the PMMA/Si substrate.

Eventually, after annealing for a long time (>12 h) at 140°C, samples on both PS/Si and PMMA/Si substrates became fairly smooth, as observed with the microscope, and cracks were essentially filled in.

Figure 15 shows, for a monolayer of 1.02-μm microspheres on a 1-mm-thick glass slide, the contents in red, green and blue averaged over an entire image (of size 50 μm × 38 μm) during an annealing experiment. The three color intensities were normalized to the whole image grayscale intensity, to avoid variations due to changes in illumination and camera gain over time. Dramatic changes in color occur just above T_g, and the three curves evolve toward asymptotic values at longer times.

The lowercase letters in Fig. 15 identify the times at which the images shown in the various panels of Fig. 16 were acquired. In Fig. 16 are shown small portions (16 μm × 16 μm) of the images used to generate Fig. 15, converted to grayscale images.

A small area of each image of the 1.02-μm microsphere monolayer on a glass slide was analyzed using the method described in Section 3. The average microsphere-to-microsphere distance and its standard deviation, as well as the average over all microspheres j of the sixfold bond orientation order parameter ψ_{6j}, are plotted on Fig. 17. The horizontal axis is the same as in Fig. 15 to facilitate comparisons. There is a gap in the data for temperatures just above T_g. In that temperature interval, it was very difficult to distinguish the individual microspheres in the microscope images. In Fig. 18 is shown a series of images that were acquired during annealing which form a sequence

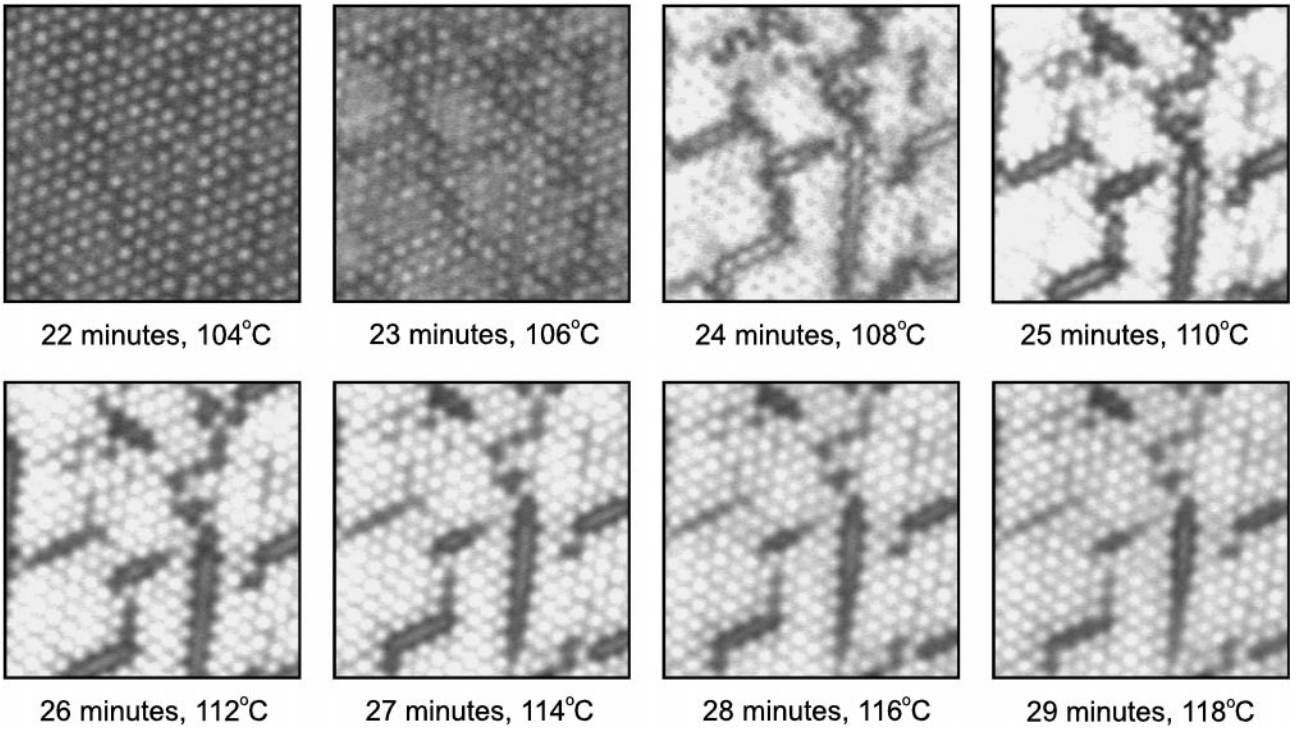

FIG. 18. Details of 1.02-μm microsphere monolayer images acquired during annealing for the times where no microsphere position information could be extracted (see Fig. 17). The color images were converted to grayscale.

spanning the interval in which no reliable microsphere position information could be extracted.

The index of refraction of the material forming the microspheres was calculated from the ellipsometric measurements that were used to characterize the microsphere material (cf. Section 2). In ramping the temperature from 60°C up to 120°C, the index of refraction goes approximately from 1.575 down to 1.552. As a result, the index of refraction of the microsphere material does not become equal to that of the glass substrate, which was measured with ellipsometry to be $(1.514 - 0.0176i)$. Therefore, index matching must be ruled out as an explanation of the difficulty in obtaining good images in the intermediate temperature range.

6. SUMMARY AND CONCLUSIONS

We have studied the self-assembly of polystyrene (PS) microspheres on both hydrophilic (glass) and hydrophobic (PS and PMMA films on Si) substrates. In particular, we have modified the self-assembly procedure to obtain reasonably well-ordered microsphere monolayers on hydrophobic substrates. We have developed an image analysis procedure for characterizing the morphology of the microsphere monolayers observed in optical micrographs, and we have used this procedure to quantify changes in the morphology that occur for annealing temperatures both above and below the glass transition temperature T_g of the PS molecules. For annealing temperatures $T < T_g$, large ordered domains in the monolayers break up into smaller regions separated by cracks, due to thermal expansion of the polymer and the attractive dispersion force between microspheres. The underlying substrate is observed to affect this process. For annealing temperatures $T > T_g$, we have observed qualitative differences in the evolution of the morphology of the microsphere monolayers on PS and PMMA substrates.

ACKNOWLEDGMENTS

We thank Dr. Alan Denton for very useful discussions, and we gratefully acknowledge the financial support of the Natural Sciences and Engineering Research Council of Canada.

REFERENCES

1. Deegan, R. D., Bakajin, O., Dupont, T. F., Huber, G., Nagel, S. R., and Witten, T. A., *Nature* **389,** 827 (1997).
2. Trau, M., Saville, D. A., and Aksay, I. A., *Science* **272,** 706 (1996).
3. Kim, E., Xia, Y., and Whitesides, G. M., *Adv. Mater*. **8,** 245 (1996).
4. Nagayama, K., *Phase Transit*. **45,** 185 (1993).
5. Bangs Laboratories, Inc., 9025 Technology Drive, Fischers, IN 46038-2886, USA.
6. Fisher Scientific, 711 Forbes Ave., Pittsburgh, PA 15219-9919, USA.
7. Denkov, N. D., Velev, O. D., Kralchevsky, P. A., Ivanov, I. B., Yoshimura, H., and Nagayama, K., *Langmuir* **8,** 3183 (1992).
8. Polymer Source, Inc., 771 Lajoie, Dorval, QC H9P 1G7, Canada.
9. WaferNet, Inc., 1785 Fox Dr., San Jose, CA 95131, USA.
10. Brochard-Wyart, F., and Daillant, J., *Can. J. Phys*. **68,** 1084 (1990).
11. Media Cybernetics, 8484 Georgia Ave., Silver Spring, MD 20910, USA.
12. Ramos, L., Lubensky, T. C., Dan, N., Nelson, P., and Weitz, D. A., *Science* **286,** 2325 (1999).
13. Aizenberg, J., Braun, P. V., and Wiltzius, P., *Phys. Rev. Lett.* **84,** 2997 (2000).
14. Crocker, J. C., and Grier, D. G., *J. Colloid Interface Sci*. **179,** 298 (1996).
15. Larsen, A. E., and Grier, D. G., *Phys. Rev. Lett.* **76,** 3862 (1996).
16. O'Rourke, J., "Computational Geometry in C." Cambridge Univ. Press, Cambridge, UK, 1994.
17. Brandrup, J., and Immergut, E. H., Eds., "Polymer Handbook," 3rd ed. Wiley, New York, 1989.
18. Milnes, A. G., and Feucht, D. L., "Heterojunctions and Metal-Semiconductor Junctions." Academic Press, New York, 1972.
19. Israelachvili, J., "Intermolecular and Surface Forces," 2nd ed. Academic Press, New York, 1998.